Ferromagnetism in Mn-doped GaAs due to substitutional-interstitial complexes

Priya Mahadevan and Alex Zunger

National Renewable Energy Laboratory, Golden, Colorado 80461, USA

While most calculations on the properties of the ferromagnetic semiconductor GaAs:Mn have focused on isolated Mn substituting the Ga site (Mn_{Ga}), we investigate here whether alternate lattice sites are favored and what the magnetic consequences of this might be. Under As-rich (Ga-poor) conditions prevalent at growth, we find that the formation energies are lower for Mn_{Ga} over interstitial Mn (Mn_i). As the Fermi energy is shifted towards the valence band maximum via external p doping, the formation energy of Mn_i is reduced relative to Mn_{Ga}. Furthermore, under epitaxial growth conditions, the solubility of both substitutional and interstitial Mn are strongly enhanced over what is possible under bulk growth conditions. The high concentration of Mn attained under epitaxial growth of p-type material opens the possibility of Mn atoms forming small clusters. We consider various types of clusters, including the Coulomb-stabilized clusters involving two Mn_{Ga} and one Mn_i. While isolated Mn_i are hole killers (donors), and therefore destroy ferromagnetism, complexes such as (Mn_{Ga}-Mn_i-Mn_{Ga}) are found to be more stable than complexes involving Mn_{Ga}-Mn_{Ga}-Mn_{Ga}. The former complexes exhibit partial or total quenching of holes, yet Mn_i in these complexes provide a channel for a ferromagnetic arrangement of the spins on the two Mn_{Ga} within the complex. This suggests that ferromagnetism in Mn-doped GaAs arises both from holes due to isolated Mn_{Ga} as well as from strongly Coulomb stabilized Mn_{Ga}-Mn_i-Mn_{Ga} clusters.

I. INTRODUCTION

The discussion[1,2] of the physics that underlies room-temperature ferromagnetism in transition-metal doped semiconductors has largely focussed on *substitutional* geometries, e.g., the Mn_{Ga} site in GaAs. Indeed, there is a well-established tradition that $3d$ impurities in III-V semiconductors are largely substitutional,[3] while in Si they are mostly interstitial.[4] Modern first-principles total-energy calculations afford testing of this classic paradigm. Recent experiments[5] find that Mn atoms occupy both substitutional as well as interstitial positions in GaAs. There have been suggestions from recent theoretical work[6] that primarily surface energetics will funnel Mn atoms in to interstitial sites from surface adatom positions. While Mn_{Ga} behaves as a hole-producing acceptor, at the interstitial site, Mn_i behaves as an electron-producing donor. Since ferromagnetism is mediated by free-carriers, Mn_i could modify the magnetic properties from the case where only substitutional Mn sites were occupied.

Using density-functional theory as implemented within plane-wave pseudopotential total energy method, we consider here bulk and epitaxial growth conditions, investigating isolated defects (Mn_{Ga} and Mn_i) and their complexes. We find that the Mn impurity in GaAs is stable in both substitutional and interstitial geometries depending on (a) the Fermi energy (which can be changed via external doping), (b) chemical potentials during growth and (c) bulk versus epitaxial growth conditions. The origin of these dependences is as follows: (a) The formation energy of impurities that are neutral with respect to the lattice site they occupy (e.g., Mn_{Ga}^0) does not depend on the Fermi energy (ϵ_F). However, the formation energy of positively charged impurities (e.g., Mn_i^{2+}) decreases as ϵ_F is shifted towards the VBM. Hence, the difference in the formation energies between Mn_i^{2+} and Mn_{Ga}^0 decreases with p-type doping, resulting in increased

solubility of interstitial Mn. (b) Substitution of Ga by Mn involves the removal of a Ga atom and the introduction of a Mn atom at the site vacated by Ga. Thus, substitution is generally enhanced under Ga-poor, Mn-rich growth conditions. On the other hand the formation energy of Mn at an interstitial site does not depend on the Ga chemical potential. Thus, one may stabilize substitutional (interstitial) doping using Ga-poor (Ga-rich) growth conditions. (c) Solid solubility can be controlled thermodynamically using epitaxial instead of bulk growth conditions.[7] The absence of a substrate under bulk growth conditions allows the growing solid as well as its possible disproportionation products to attain their free-standing lattice geometry. This is the case when the growth takes place from the melt as in Bridgman growth. Then, if phase separation occurs, the precipitate will take up its most stable crystal structure, i.e., MnAs in the NiAs structure. In contrast, under thin-film epitaxial growth conditions (as in molecular beam epitaxy, metal-organic chemical vapor deposition) competing phases such as phase separated MnAs are forced to be coherent with the GaAs substrate. As zinc-blende MnAs strained on GaAs is less stable than the NiAs phase of MnAs, phase separation is more costly under coherent epitaxial conditions, and one expects[7] less phase separation, hence enhanced solubility. We find the following.

(i) Substitutional Mn has two stable charge states: neutral (Mn_{Ga}^0) and negatively charged (Mn_{Ga}^-) charge state which have 1 and 0 holes, respectively. The calculated acceptor transition $E(0/-)$ between these states occurs at $E_v + 0.13$ eV, in good agreement with the experimental value of $E_v + 0.11$ eV.[8] Here E_v corresponds to the valence band maximum of the host material.

(ii) The interstitial sites that Mn can occupy have either tetrahedral (coordinated to four As or four Ga atoms) or hexagonal symmetry. We find that Mn at the tetrahedral interstitial site coordinated by As is more stable than that coordi-

nated by Ga, and exhibits a single charge state Mn^{2+} for all values of the Fermi energy. The $(0/+)$ and $(+/2+)$ donor transitions are found to lie inside the conduction band, so, isolated Mn_i produce electrons that will compensate the holes created by Mn_{Ga}.

(iii) Under *bulk* growth conditions, the formation energy per Mn of substitutional Mn is $\Delta H(Mn_{Ga}^0) = 0.91 + \mu_{Ga} - \mu_{Mn}$ eV $= 0.17 - \mu_{As} - \mu_{Mn}$ eV, whereas interstitial Mn has $\Delta H(Mn_i^{2+}) = 0.55 - \mu_{Mn} + 2\epsilon_F$ eV per Mn. Here ϵ_F is the Fermi energy measured with respect to the valence band maximum of the host material, and μ_{As} and μ_{Mn} are the chemical potentials of As and Mn respectively. If we use maximally As-rich growth conditions ($\mu_{As} = 0$ eV) and $\mu_{Mn} = \Delta H(MnAs)$, then we find $\Delta H(Mn_{Ga}^0) = 0.91$ eV. As one dopes the sample p-type and ϵ_F approaches the VBM ($\epsilon_F = 0$), the energy difference between the formation energies of Mn_{Ga}^0 and Mn_i^{2+} reduces to 0.38 eV. It could decrease even further if ϵ_F penetrates the valence band with doping, or if the growth conditions are made less As rich. The interstitial concentration is then expected to further increase. Recent experiments[9] which use Ga-rich conditions for growth could be interpreted as a confirmation of this.

(iv) Under *epitaxial* growth conditions, the formation energies of both substitutional and interstitial Mn decrease by 0.74 eV/Mn, so their concentrations increase concomitantly leading to the possibilities of clusters. There is strong coulomb interactions between the oppositely charged constituents involving two substitutional (Mn_{Ga}) and one interstitial (Mn_i); the cluster Mn_{Ga}-Mn_i-Mn_{Ga} is thus strongly stabilized and found to be more stable under p-type conditions than clusters involving three Mn_{Ga}. Epitaxial growth conditions increases the solubility of such Mn_{Ga}-Mn_i-Mn_{Ga} clusters, with formation energy of $-0.15 + \epsilon_F$ eV per cluster for the $Q = +1$ charge state under As-rich conditions and $\mu_{Mn} = \Delta H(MnAs)$.

(v) The presence of interstitial Mn in the Mn_{Ga}-Mn_i-Mn_{Ga} cluster provides a channel for the spins on the two substitutional Mn to align ferromagnetically even when there are no free carriers present in the cluster. We therefore conclude that ferromagnetism in GaAs:Mn can arise both from holes induced by isolated substitutional Mn atoms discussed previously[1] as well as from charge compensated substitutional-interstitial clusters.

II. METHOD OF CALCULATION

The formation energy for a defect comprising of atoms α in the charge state q was computed using the density functional supercell method using the expression[10]

$$\Delta H_f^{\alpha,q}(\epsilon_F, \mu) = E(\alpha) - E(0) + \sum_\alpha n_\alpha \mu_\alpha^a + q(E_v + \epsilon_F),$$

(1)

where $E(\alpha)$ and $E(0)$ are the total energies of a supercell with and without the defect α respectively. n_α denotes the number of atoms of defect α transferred in or out of the reservoir (equal to 1 for an atom removed, and to -1 for an atom added), while μ_α^a denotes their chemical potentials.

Total energies. The total energies of the charged supercells were computed by compensating any additional charge on the impurity atom by a uniform jellium background and have been corrected for interactions between charges in neighboring cells using the Makov-Payne correction.[11] For isolated defects we used both the monopole as well as quadrupole corrections, while for composite defects we have added only the monopole correction to the total energy assuming all the charge to be localized at a single point. We use the static dielectric constant of GaAs (12.4).[12] The quadrupole moment of the isolated defects was calculated as the difference between the moments of the supercell with the charged defect and that with the neutral defect.

Transition energies. The defect transition energy $\epsilon(q, q')$ is the value of the Fermi energy ϵ_F at which $\Delta H^{\alpha,q}(\epsilon_F) = \Delta H^{\alpha,q'}(\epsilon_F)$. The zero of the Fermi energy is chosen as the valence band maximum E_v of the pure host at the Γ point.

Chemical potential limits. As the reservoir supplying the atoms could be elemental solids, or compounds formed from the elements, we express μ_α^a as the sum of the energy of the element in its most stable structure μ_α^s, and an additional energy μ_α, i.e., $\mu_\alpha^a = \mu_\alpha^s + \mu_\alpha$. The required ranges of μ_α are determined by $\mu_{Ga} \leq 0$, $\mu_{Mn} \leq 0$, $\mu_{As} \leq 0$ (no precipitation of solid elements), and by the formation energies of GaAs, and MnAs. The allowed values of chemical potential are such that GaAs is stable, i.e., $\mu_{Ga} + \mu_{As} = \Delta H_f(GaAs)$, the latter being the formation energy of zinc-blende GaAs. Further, as Mn should not precipitate as MnAs, we restrict $\mu_{Mn} + \mu_{As} < \Delta H_f(MnAs)$, the formation energy of MnAs in its most stable (NiAs) structure. For epitaxial growth conditions, the formation energy of zinc-blende MnAs lattice-matched to GaAs is considered. In this case we calculate the epitaxial formation energy, $\Delta H_f(MnAs)_{epi}$, forcing the in-plane lattice constant of MnAs to become equal that of GaAs, while the out-of-plane lattice constant c is allowed to vary. For coherent epitaxial growth the condition that MnAs should not form during incorporation of Mn in GaAs becomes $\mu_{Mn} + \mu_{As} < \Delta H_f(MnAs)_{epi}$.

The energies $E(\alpha)$, $E(0)$, $\Delta H_f(GaAs)$, $\Delta H_f(MnAs)$, $\Delta H_f(MnAs)_{epi}$, and μ_α are calculated within the density functional formalism, through the momentum-space pseudopotential total energy representation,[13] using ultrasoft pseudopotentials.[14] The GGA-PW91 version of the exchange-correlation functional[15] was used and no correction for the band gap underestimation was made. The calculations were performed over a Monkhorst-Pack $4 \times 4 \times 4$ k-point grid for 64 (Ref. 16) and 216 atom supercells of GaAs using VASP.[17] Changing the k-point mesh from $2 \times 2 \times 2$ to $4 \times 4 \times 4$ changed the formation energies by ~ 20 meV. Larger 256-atom supercells with $1 \times 1 \times 2$ k points were used for the calculations with clusters to ensure a larger separation between clusters. We used a plane wave cutoff of 227.2 eV for these calculations. Increasing the cutoff to 300 eV, changed the formation energies by ~ 10 meV. As the lattice constant of the supercell was kept fixed at the GGA optimized value for GaAs of $a = 5.738$ Å,[18] the internal coordinates were optimized. Our calculated (experimental) formation energies are $\Delta H_f(GaAs) = -0.74 (-0.74)$,

TABLE I. Acceptor transitions, Formation energies of Mn_{Ga} and Mn_i for 64- and 216-atom supercells of GaAs, with and without charge corrections.

Quantity	64-atom cell with (without) charge correction (in eV)	216-atom cell with (without) charge correction (in eV)
$Mn_{Ga}(0/-)$	0.183 (0.094)	0.133 (0.068)
$\Delta H_f(Mn_i^{2+}) - \Delta H_f(Mn_{Ga}^0)$[a]	0.382 (0.016)	0.430 (0.17)
$\Delta H_f(Mn_{Ga}^0)$	$0.908 + \mu_{Ga} - \mu_{Mn}$	$1.261 + \mu_{Ga} - \mu_{Mn}$

[a] $\mu_{Mn} = \Delta H(MnAs), \mu_{As} = 0, \epsilon_F = 0$

$\Delta H_f(MnAs) = -0.74\ (-0.61)$ eV and $\Delta H_f(MnAs)_{epi} \sim 0$ eV. For elemental Mn we assume the nonmagnetic fcc structure,[20] while for elemental Ga, we assume the base-centered orthorhombic structure.

The charge corrected[11] Mn_{Ga} (0/-) transition as well as the difference in formation energies between Mn_{Ga}^0 and Mn_i^{2+} are given in Table I for supercell sizes of 64 and 216 atoms. We see that changing the supercell size from 64 to 216 atoms lowers the acceptor energy by 30–50 meV and stabilizes Mn_{Ga}^0 over Mn_i^{2+} by 50–150 meV. The charge correction increases the acceptor energy by 60–90 meV and stabilizes Mn_{Ga}^0 over Mn_i^{2+} by 250–350 meV.

III. RESULTS

A. Isolated substitutional Mn on the Ga site of GaAs

Figure 1 describes the formation energy $\Delta H(Mn_{Ga}^0)$ of neutral substitutional Mn in GaAs as a function of the chemical potentials μ_{As} and μ_{Mn}. The shaded areas denote chemical potentials that produce unwanted products: (i) When μ_{As} becomes greater than zero (the cohesive energy of solid As) we have precipitation of elemental As as shown on the left hand side of Fig. 1. (ii) In the opposite limit, when μ_{As} takes more negative values than the formation energy $\Delta H(GaAs)$, we have maximally As-poor conditions and the host itself becomes unstable, as shown on the right hand side of Fig. 1. (iii) The diagonal lines in the main body of Fig. 1 denote different values of μ_{Mn}. When the chemical potential of Mn becomes greater than zero (the cohesive energy of solid Mn), metallic Mn will precipitate as shown in the bottom right corner of Fig. 1. Conversely, (iv) when μ_{Mn} becomes equal or larger than $\Delta H(MnAs) - \mu_{As}$, we will precipitate a secondary phase of MnAs. Clearly, since $\mu_{Ga} + \mu_{As} = \Delta H(GaAs)$ and $\mu_{Mn} + \mu_{As} < \Delta H(MnAs)$, one can keep the latter inequality even for moderately negative values of μ_{Mn}, provided that μ_{As} is adjusted. The lines in Fig. 1 show that the lowest $\Delta H(Mn_{Ga}^0)$ value is 0.91 eV (circle at bottom left corner). This can be attained at $\mu_{As} = 0$ (maximally As-rich); $\mu_{Mn} = \Delta H(MnAs)$. Alternatively, the same solubility can be attained for less rich-As conditions, but richer Mn conditions, e.g., for $\mu_{As} = -0.5$ eV and $\mu_{Mn} = -0.24$ eV.

Having described in Fig. 1 the stability of the *neutral* substitutional, we next describe in Fig. 2 the stability of the *charged* substitutionals. Here we chose the chemical potentials $\mu_{As} = 0$, $\mu_{Mn} = \Delta H(MnAs)$ (denoted by the circle in Fig. 1) and vary the Fermi energy. We see that for *p*-type
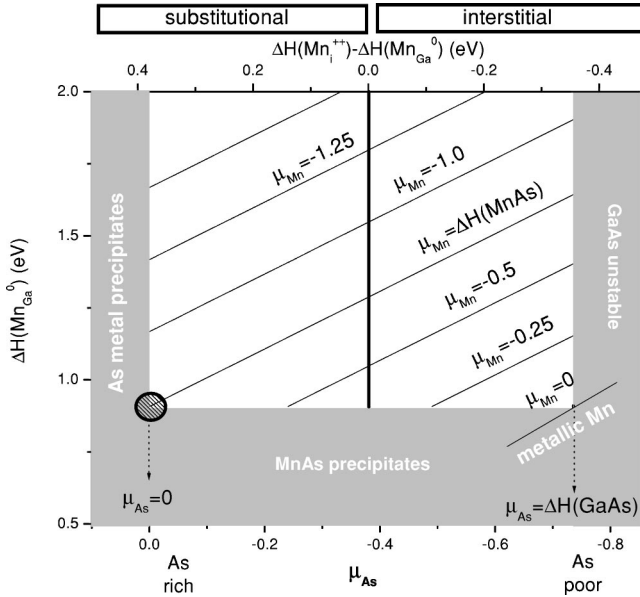

FIG. 1. The formation energy of Mn_{Ga}^0 (left y axis) as well as the difference in formation energies of Mn_i^{2+} and Mn_{Ga}^0 (top x axis) are plotted as a function of μ_{As} (bottom x axis) for different values of μ_{Mn}. Here ϵ_F is fixed at the VBM of the host. Regions where there is precipitation of the elemental solids as well as MnAs are also shown.
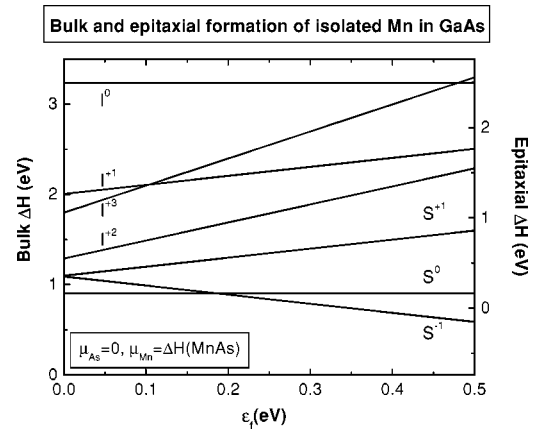

FIG. 2. The bulk (left y axis) as well as epitaxial (right y axis) formation energies for different charge states of isolated substitutional (S) and isolated interstitial (I) Mn calculated for a 64-atom supercell under As-rich conditions. Acceptor transition for 216-atom supercell (Table I) is $E_v + 0.13$ eV. The chemical potentials are fixed at the points corresponding to the circle shown in Fig. 1.
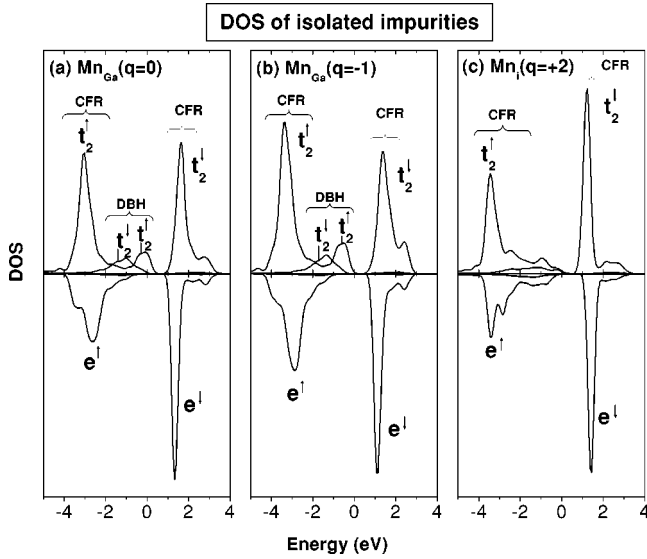
FIG. 3. The t_2 (upper panel) and e (lower panel) projected contributions to the Mn d projected partial DOS (a) for the $q=0$ and (b) -1 states of Mn_{Ga} as well as (c) the $q=+2$ charge state of Mn_i.
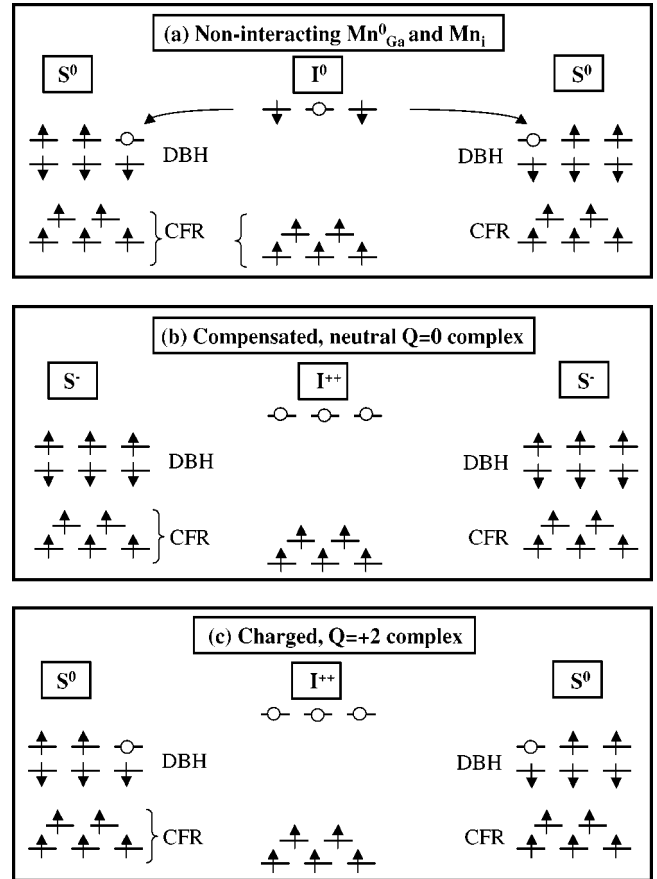

FIG. 4. Schematic energy-level diagram for (a) neutral noninteracting substitutional (S) and interstitial (I) Mn impurities, (b) the compensated S-I-S complex and (c) the doubly charged S-I-S complex involving two substitutional and one interstitial Mn, where Q is the total charge of the complex. Open circles denote holes.

conditions, the lowest energy charge state is Mn_{Ga}^0, whereas for higher Fermi energy the stablest charge state is Mn_{Ga}^-. Table I gives the (0/-) acceptor transition energy calculated with various supercell sizes with and without charge correction. The most converged (0/-) transition energy calculated for the 216 atom cell and corrected for charge interactions is $E_v + 0.13$ eV, in good agreement with the measured value of $E_v + 0.11$ eV.[8] Fig. 2 shows that under epitaxial conditions (right y axis), the formation energy of Mn_{Ga}^0 is lowered by 0.74 eV.

We next describe the electronic structure of Mn_{Ga}. In Figs. 3(a) and 3(b) we show the Mn d projected partial density of states (PDOS) for two charge states of substitutional Mn. The main features can be understood as arising from the hybridization between the anion dangling bonds generated by a Ga vacancy and the d levels on the Mn ion placed at the vacant site.[3] The Mn d ion levels are split by the tetrahedral crystal field into $t_2(d)$ and $e(d)$. Exchange interactions further split these levels into spin-up ($\uparrow$) and spin-down ($\downarrow$) levels. The $t_2(d)$ levels on the Mn atom hybridize with the levels with the same symmetry on the As dangling bonds, while the $e(d)$ levels have no other states available for significant coupling.[3] Because the location of the Mn ion d levels is below the dangling bond levels, after hybridization, the deeper bonding t_2 states have dominantly Mn d character (referred to as CFR: "crystal field resonance"), while the higher antibonding t_2 states have dominantly As p character (refered to as DBH: "dangling bond hybrid"). These interactions lead to the energy level diagram depicted schematically on the left-hand side of Fig. 4 showing a fully occupied, Mn-localized up-spin CFR of t_2 and e symmetries. At a higher energy we have the up- and down-spin DBH states with t_2 symmetry. Because of the location of the Ga vacancy states $t_2(p)$ between the exchange split $t_2(d)$ states on the Mn, a negative exchange splitting is induced as a result of

hybridization on the DBH states[21] with $t_{DBH}^{\downarrow}$ below $t_{DBH}^{\uparrow}$. As a result, the neutral substitutional defect Mn_{Ga}^0 has the electron configuration $[t_{\uparrow}^3 e_{\uparrow}^2]_{CFR} (t_{\downarrow}^1 t_{\uparrow}^2)_{DBH}$, with a total magnetic moment $\mu = 4\mu_B$, and a hole in the $t_{DBH}^{\uparrow}$ orbital. This configuration corresponds to the multiplet $^5T_2$ as observed in electron paramagnetic resonance (EPR) experiments.[22] The partial occupancy of the negative exchange-split DBH states stabilizes the ferromagnetic state over the antiferromagnetic state.[21]

B. Isolated interstitial Mn

Mn interstitial can occupy a site with tetrahedral symmetry (coordinated by four As or four Ga atoms) or a site with hexagonal symmetry. We have calculated the total energies of Mn at these positions in a 64-atom cell of GaAs, and the results for the tetrahedral interstitial sites are given in Table II. The tetrahedral interstitial $Mn_i(As)$ coordinated by four As atoms is more stable than the one coordinated by four Ga atoms, with the difference being 0.16, 0.31, and 0.31 eV for charge states $q=1$, 2, and 3. In contrast, the hexagonal interstitial has 0.62 eV higher total energy than the most stable $Mn_i^{2+}(As)$. Experimentally, the presence of interstitial Mn

TABLE II. The formation energy for different charge states of isolated substitutional (Mn_{Ga}) as well as interstitial Mn coordinated to four As atoms $[Mn_i(As)]$ or to four Ga atoms $[Mn_i(Ga)]$, where μ_α denotes the chemical potential for atom α.

Charge state	Formation energy	
	T_d $Mn_i(As)$	T_d $Mn_i(Ga)$
-1	3.81-μ_{Mn}-ϵ_F	
0	2.45-μ_{Mn}	
$+1$	1.19-μ_{Mn}+ϵ_F	1.35-μ_{Mn}+ϵ_F
$+2$	0.18-μ_{Mn}+$2\epsilon_F$	0.49-μ_{Mn}+$2\epsilon_F$
$+3$	0.24-μ_{Mn}+$3\epsilon_F$	0.55-μ_{Mn}+ϵ_F

was detected by an analysis of the EPR spectrum[23] as well as by Rutherford back scattering.[5] The distinction between the two types of T_d interstitial sites (Mn-next to As vs Mn-next to Ga) is difficult to determine experimentally and involved an analysis of the experimentally measured contact interaction in terms of the covalency of the Mn-X bond. This analysis suggested that $Mn_i(Ga)$ was more stable, while our total energy calculations suggest that $Mn_i(As)$ is more stable.

The formation energy of various charge states of interstitial Mn is shown in Fig. 2 for $\mu_{As}=0$ and $\mu_{Mn}=\Delta H(MnAs)$. We see that the stable charge state is Mn_i^{2+} for the full range of Fermi level, with maximum stability at $\epsilon_F=0$. To compare the relative stability of Mn_i^{2+} at $\epsilon_F=0$ with substitutional Mn_{Ga}^0, we show in the upper scale of Fig. 1 the difference $\Delta H(Mn_i^{2+}) - \Delta H(Mn_{Ga}^0)$ between the formation energies of interstitial and substitutional Mn. We see that substitutional Ga is stabler on the left hand side of the figure, i.e., sufficiently As-rich, whereas interstitial Mn is stabler at the right hand side of the figure, i.e., sufficiently As-poor. The energy difference is

$$\Delta H(Mn_i^{2+}) - \Delta H(Mn_{Ga}^0) = 0.38 + \mu_{As} + 2\epsilon_F .$$

For $\mu_{As}=0$, the substitutional Mn are stabler by 0.38 eV, while for moderately As-rich conditions, say $\mu_{As}=-0.4$ eV, both defects have comparable formation energies.

These results are in agreement with recent experiments using liquid phase epitaxy[9] to introduce Mn in GaAs. Experimentally a decrease in hole concentration is found as the Mn concentration is increased. Under the Ga-rich growth conditions used, As antisites are not expected to be the dominant source of the observed compensation. Hence the major source of compensation is believed to come from Mn_i as expected for Ga-rich conditions from Fig. 1.

We next examine the electronic structure of Mn at a tetrahedral interstitial site. When Mn occupies a tetrahedral interstitial position, five of the seven electrons occupy the $t_\uparrow e_\uparrow$ CFR levels, with the remaining two going into the down-spin $t_\downarrow$ levels. This is evident from the PDOS for the doubly ionized Mn_i^{2+} shown in Fig. 3(c), where Mn_i^{2+} is found to have the configuration $[t_\uparrow^3 e_\uparrow^2]_{CFR}$ with a magnetic moment of $\mu=5\mu_B$. The central panel of Fig. 4(a) shows schematically the levels of Mn_i. As the (0/+) and (+/2+) transitions are
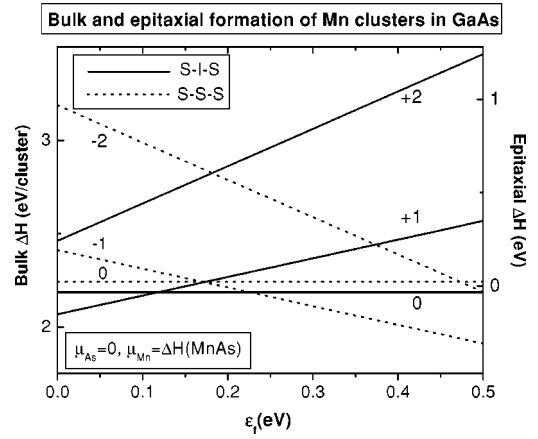

FIG. 5. The bulk (left y axis) as well as epitaxial (right y axis) formation energies for different charge states of complexes involving two substitutional and one interstitial Mn compared with three substitutional Mn calculated for a 64-atom supercell under As-rich conditions. The chemical potentials are fixed at the points corresponding to the circle shown in Fig. 1.

calculated to lie inside the GaAs conduction band (Fig. 2), we conclude that Mn_i produce free electrons in GaAs.

C. Clusters of substitutional Mn

Having dealt with the isolated limit, we investigated whether Mn atoms show a tendency to cluster. Recent experiments[24] on dilute magnetic semiconductors have found a strong tendency of the doped transition metal atoms to cluster and there has been some theoretical work[2] to support such observations. We consider As-centered clusters $[(As)Mn_nGa_{4-n}]$ with $n=0, 1, 2, 3$, and 4.

Figure 5 shows the formation energy of clusters made of three substitutional Mn atoms (S-S-S) at lattice locations $(0,0,0)$, $(a/2,a/2,0)$, and $(0,a/2,a/2)$ in the 64-atom supercell. This corresponds to the $n=3$ cluster. Here a is the cubic lattice constant of GaAs. We see that the neutral cluster $(3\ Mn_{Ga})^0$ having three holes is stable under p-type conditions, whereas the charged cluster $(3Mn_{Ga})^-$ with two holes is more stable above $\epsilon_F=0.15$ eV. The energies of the complex with $3(Mn_{Ga})^0$ is $2.2+3(\mu_{Ga}-\mu_{Mn})$ eV while that of three noninteracting Mn_{Ga} in their lowest energy charge state is $2.71+3(\mu_{Ga}-\mu_{Mn})$ eV. For epitaxial conditions $\Delta H_{epi}=0.02+3(\mu_{Ga}-\mu_{Mn})$ eV/cluster. Thus, as the formation energy is very low, the tendency for the Mn atoms to cluster is strongly enhanced under epitaxial growth conditions.

In order to obtain a measure of the tendency to cluster, we calculate the clustering energy. The "clustering energy" $\delta(n)$ is defined as the energy difference between n substitutional Mn atoms surrounding an As site $[(As)Mn_nGa_{4-n}; \ 0\leqslant n\leqslant 4]$ and n isolated well-separated constituents. Thus, $\delta E(n)=[E(n)-E(0)]-n[E(1)-E(0)]$, where $E(n)$ is the total energy of the supercell with As-centered clusters of n Mn atoms. We find that $\delta E(n)=-228, -482$ and -794 meV per cluster of $n=2, 3$, and four Mn atoms for a 64-atom supercell. The clustering energy changed to -519 and -1069 meV for

clusters involving two and three Mn atoms in a 256-atom supercell. These results indicate a strong tendency for the neutral substitutional Mn atoms to form clusters.

D. Neutral complexes of Mn_{Ga} and Mn_i

We considered the defect complex formed between Mn_{Ga} (S) and interstitial Mn_i (I) denoted as $(S-I-S)^Q$, where Q is the total charge of the complex. Although our results for Mn_i (Table I) suggest that $Mn_i(As)$ is more stable than $Mn_i(Ga)$, we find that in the neutral complex (S-I-S), the energies for Mn_i at either interstitial site are comparable. We now discuss the cluster which has Mn_{Ga} at $(0,0,0)$ and $(a/2,a/2,0)$ and Mn_i at $(a/2,0,0)$ in the 64-atom supercell of GaAs. We see in Fig. 5 that S-I-S exists in two charge states: When the Fermi energy is below $E_v + 0.1$ eV we have the stable structure is $(S-I-S)^{1+}$, whereas when ϵ_F is above it, the stable structure is the neutral $(S-I-S)^0$. Thus, the donor transition for the cluster is at $E_v + 0.1$ eV. Figure 5 also shows that for Fermi levels below $E_v + 0.22$ eV, the S-I-S complex is more stable than the S-S-S complex. As for the interaction energy of the components of the complex: the formation energy of the noninteracting neutral components of the complex is $2E(Mn_{Ga}^0) + E(Mn_i^0) = 4.31 + 2\mu_{Ga} - 3\mu_{Mn}$ eV per 3 impurities, while the formation energy of the *interacting* neutral complex is $1.41 + 2\mu_{Ga} - 3\mu_{Mn}$ eV. This represents a ~ 2.9eV per three impurities stabilization over the noninteracting, neutral defects. The energy of the neutral complex measured with respect to the stablest lattice site occupied by isolated Mn under particular experimental conditions is found to be -574 meV for $\mu_{As} = 0$ eV, $\mu_{Mn} = \Delta H(MnAs)$ and $\epsilon_F = 0$ eV. Hence this complex is strongly stabilized.

The reasons for the stability of the $(S-I-S)^0$ complex can be appreciated from Fig. 4(a). Upon bringing together $2Mn_{Ga}^0$ with Mn_i^0, one electron drops from the higher energy $t_\downarrow^{CFR}$ level of Mn_i to the lower energy $t_\uparrow^{DBH}$ level of each substitutional site, resulting in $[t_\uparrow^3 e_\uparrow^2]_{CFR}(t_\uparrow^3 t_\uparrow^3)_{DBH}$ configuration at each Mn_{Ga} site [Fig. 4(b)] which corresponds to Mn_{Ga}^-. These conclusions are evident from our calculated density of states (DOS) of the S-I-S complex, projected on the I and S sites shown in Fig. 6. We find that for both $Q = 0$ [Fig. 6(a)] and $Q = 2$ [Fig. 6(b)] the I site has the configuration $[t_\uparrow^3 e_\uparrow^2]_{CFR}$ or "$d_\uparrow^5$." This substitutional-to-interstitial charge transfer lowers the energy of the complex by twice the separation between $t_\downarrow^{CFR}$ level of Mn_i and $t_\uparrow^{DBH}$ level of Mn_{Ga}. Furthermore, it creates a favorable Coulomb attraction between the components $S^- - I^{2+} - S^-$ of the complex. This energetically favorable substitutional-interstitial association reaction then eliminates the holes that were present in isolated substitutional Mn_{Ga} and could explain the puzzling observation[25] of the existence of a far lower concentration of holes than Mn in GaAs. Alternate explanations such as the presence of As antisites[28] as well as the presence of Mn atoms connected to six As atoms (as in the NiAs structure) have been offered. However, samples have been prepared where the concentration of As antisites is too low to
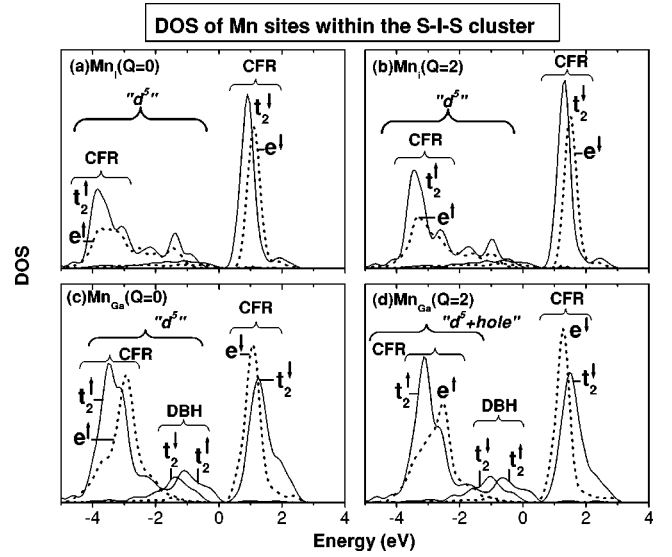

FIG. 6. The t_2 (solid line) and e (dotted line) projected contributions to the Mn d projected partial density of states for $Q = 0$ (left panels) and $Q = +2$ (right panels) of the complex projected onto Mn_i (top panels) and Mn_{Ga} (bottom panels).

explain the observed compensation of holes. Further, six-fold coordinated Mn atoms have not been observed in Mn doped GaAs samples.[26]

E. Ferromagnetism of the $(S-I-S)^0$ complex

The neutral complex has two Mn_{Ga}^- and one intervening "$d_\uparrow^5$" interstitial. We find that a ferromagnetic arrangement between Mn_{Ga} is favored in the complex $(Mn_{Ga}^- - Mn_i^{2+} - Mn_{Ga}^-)^0$ by 176 meV. In contrast, our calculations for two Mn_{Ga}^- atoms *without* the intervening interstitial atom finds that an *antiferromagnetic* arrangement of spins on the substitutional Mn atoms is favored by 108 meV. Thus Mn_i is responsible for mediating a ferromagnetic interaction between Mn_{Ga}^0.

How does the presence of the interstitial Mn mediate the alignment of spins on the substitutional Mn? There are three possible arrangements for the spins on the Mn atoms making up the neutral complex - $(S^\uparrow I^\uparrow S^\uparrow)^0$, $(S^\uparrow I^\downarrow S^\uparrow)^0$ and $(S^\uparrow I^\downarrow S^\downarrow)^0$. From our total energy calculations we find that the energy for the configurations $(S^\uparrow I^\uparrow S^\uparrow)^0$ and $(S^\uparrow I^\downarrow S^\downarrow)^0$ are higher by 563 and 176 meV, respectively, than the energy, E_0, of the ground state $(S^\uparrow I^\downarrow S^\uparrow)^0$. (The energies changed marginally to 602 and 192 meV, respectively, when we increased the supercell size to 256 atoms.) The stabilization of the $S^\uparrow I^\downarrow S^\uparrow$ magnetic arrangement can be understood using simple arguments: In the configuration $(S^\uparrow I^\uparrow S^\uparrow)^0$, as one spin channel is completely filled, there is no channel of hopping available for the electrons to delocalize and lower their energy. Thus, this is a high energy spin configuration with energy $E_0 + 563$ meV. In contrast, in the configuration $(S^\uparrow I^\downarrow S^\downarrow)^0$, two channels of hopping are present; the first between the electrons on $S^\uparrow$ and $S^\downarrow$, and the second between those on $S^\uparrow$ and $I^\downarrow$. This configuration is found to have the energy, $E_0 + 176$ meV. Likewise, the configuration $(S^\uparrow I^\downarrow S^\uparrow)$ which has
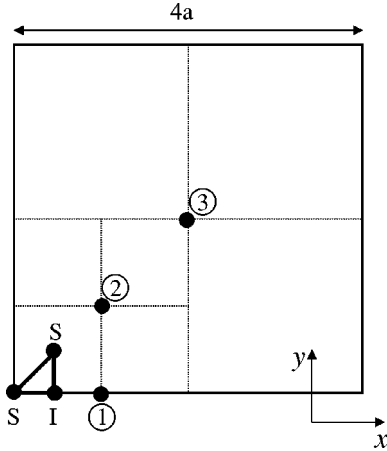
FIG. 7. A single face of the 256-atom supercell of GaAs used in our calculations, where a is the cubic cell dimension. Positions 1, 2, and 3 considered for the isolated Mn_{Ga} with respect to the cluster whose components are labeled S and I.

energy E_0 has two channels of hopping present between S and I. The dominant factor in determining the configuration which has the lowest energy are the hopping matrix elements - $V_{S,I}$ between S and I and $V_{S,S}$ between the two S's. To a first approximation, these hopping matrix elements are determined by the separation between the atoms involved. As the distance between the two substitutional Mn atoms is $\sqrt{2}$ times the distance between S and I, the effective hopping matrix element between S is smaller. Hence the presence of an intervening Mn_i provides a channel for the ferromagnetic arrangement of spins between two Mn_{Ga} even in the neutral charge-compensated complex. In contrast, the presence of a closed shell donor such as As_{Ga} between two Mn_{Ga} gives rise to an antiferromagnetic (or weakly ferromagnetic) interaction between Mn_{Ga}.

How does the presence of the interstitial affect long-range ferromagnetism? In order to investigate this we introduced a hole-producing, isolated substitutional Mn atom at different lattice locations, indicated in Fig. 7, and investigated whether the spin on this isolated substitutional Mn atom prefers to align parallel or antiparallel with respect to the spins on the substitutional Mn atoms within the S-I-S cluster. We find that the substitutional Mn likes to align ferromagnetically with the Mn_{Ga} of the cluster by 147, 214, and 81 meV, respectively, for positions 1, 2, and 3 (see Fig. 7). Hence the presence of the interstitial Mn forces a hole which is located ~ 12 Å from the S-I-S cluster to align ferromagnetically and therefore contributes to the long-ranged ferromagnetism observed in these systems.

As discussed earlier, the basic electronic structure of substitutional Mn in GaAs can be understood as arising from the hopping interaction between the Mn d states and the As p dangling bond states. Therefore, the coupling between two Mn atoms is through the As p states. It is strongest along the directions in which the "p-d" coupling of the Mn with the As states is the largest and decreases with distance along that direction. When there is a hole, the antibonding $t_2^\uparrow$ orbitals are partially occupied, and there is ferromagnetism. Hence in Fig. 7 spins on the Mn atoms at sites 2 and 3 prefer to align

ferromagnetically with the spins on S when there is partial compensation. This could happen either because the S-I-S cluster is totally compensated, and a hole exists on the Mn at sites 2/3 or the S-I-S cluster is partially compensated. The mechanism stabilizing the ferromagnetic coupling between S and site 1 is the same as what we discussed for the $(S-I-S)^0$ complex earlier and exists even when there is total compensation.

F. Charged Mn_{Ga}-Mn_i-Mn_{Ga} complexes

While the neutral complex has no holes, the $Q=+1$ and $+2$ complexes have one and two holes respectively (Fig. 4(c)) and a net magnetic moment of $4\mu_B$ and $3\mu_B$ respectively. For $Q=+2$, Mn_{Ga} adopts the configuration Mn_{Ga}^0 [Fig. 4(c)]. We find that $(Mn_{Ga}$-Mn_i-$Mn_{Ga})^{2+}$ prefers the ferromagnetic arrangement of spins on Mn_{Ga} by 286 meV, similar to the ferromagnetic preference (~ 305 meV) of Mn_{Ga}^0-Mn_{Ga}^0 pair without an intervening Mn_i. These results suggest the surprising fact that the spins on Mn_{Ga} align ferromagnetically in the charged complexes, almost as if Mn_i did not exist. The number of holes in the cluster is the same as the number in the pair, though the number of Mn atoms are different. This is in agreement with the experimental observation[27] where above a critical concentration of Mn, both the number of holes as well as the ferromagnetic transition temperature remain constant, while the magnetic moment per Mn atom decreases.[27] The magnetic moments that we obtain for the $Q=+1$ and $+2$ charge states translate into average moments of $1.33\mu_B$ and $1\mu_B$ per Mn, while the uncompensated pair of Mn_{Ga} have a magnetic moment of $4\mu_B$ per Mn. In this regime where the T_c is found to saturate, the average magnetic moment per Mn is found to vary from $\sim 3\mu_B$ at a Mn concentration of 5.54% to 1.74 at 8.3%.

Recent experiments[29] find that the T_c of the as-grown samples increased after annealing. This was interpreted as the migration of FM-reducing *interstitial* Mn to FM-enhancing *substitutional* positions. We investigated which clusters could break by annealing and promote ferromagnetism. As the S-I-S complexes are rather strongly bound with respect to their constituents, we investigated instead complexes S-I, which are bound weakly (~ -196 eV in the $+1$ charge state for μ_{As}, $\mu_{Mn}=\Delta H(MnAs)$ and $\epsilon_F = 0$ eV). We find an antiferromagnetic spin arrangement in all $Q=0,+1,+2$, and $+3$ charge states considered. Thus, when these weakly bound S-I clusters are broken, depending on the charge state, there could be an increase in the number of holes and consequently the ferromagnetic transition temperature. On the other hand, S-I-S clusters appear to be stable and hence do not disintegrate under annealing.

IV. SUMMARY

Under As-rich conditions, Mn prefers to substitute the Ga site. As the growth conditions become less As-rich, or as extrinsic doping pushes ϵ_F towards and even below the VBM, the formation energy of interstitial Mn becomes competitive with that of substitutional Mn. Under coherent epitaxial growth conditions, when MnAs precipitates are forced

to be coherent with the zinc-blende lattice, the formation energy of both substitutional and interstitial decrease. At this point, the solubility is large enough to form clusters. We find that S-I-S clusters are more stable than S-S-S clusters. S-I-S clusters are found to be strongly bound with respect to their constituents and exhibit partial or total hole compensation. While isolated Mn_i behaves like a hole killer and is expected to destroy ferromagnetism, in $(Mn_{Ga}-Mn_i-Mn_{Ga})^0$, the Mn_i is found to mediate the ferromagnetic arrangement of spins on Mn_{Ga}. The charged complex $(Mn_{Ga}-Mn_i-Mn_{Ga})^{2+}$ has a similar ferromagnetic stabilization energy on the two Mn_{Ga} sites as in a $Mn_{Ga}^0-Mn_{Ga}^0$ cluster without Mn_i *almost as if* Mn_i *did not exist*. Thus ferromagnetism in Mn doped GaAs arises from holes due to substitutional Mn_{Ga}, as well as from $Mn_{Ga}-Mn_i-Mn_{Ga}$ complexes.

ACKNOWLEDGMENTS

[1] T. Dietl, H. Ohno, F. Matsukura, J. Cibert, and J. Ferrand, Science **287**, 1019 (2000); S. Sanvito and N.A. Hill, Phys. Rev. B **63**, 165206 (2001).
[2] M. van Schilfgaarde and O.N. Mryasov, Phys. Rev. B **63**, 233205 (2001).
[3] A. Zunger in *Solid State Physics*, edited by F. Seitz, H. Ehrenreich, and D. Turnbull (Academic Press, New York, 1986), Vol. **39**, p. 275.
[4] G.W. Ludwig and H.H. Woodbury in *Solid State Physics* (Academic Press, New York, 1962), Vol. **13**, p. 223.
[5] K.M. Yu, W. Walukiewicz, T. Wojtowicz, I. Kuryliszyn, X. Liu, Y. Sasaki, and J.K. Furdyna, Phys. Rev. B **65**, 201303(R) (2002).
[6] S.C. Erwin and A.G. Petukhov, Phys. Rev. Lett. **89**, 227201 (2002).
[7] A. Zunger and D.M. Wood, J. Cryst. Growth **98**, 1 (1989).
[8] J. Schneider, U. Kaufmann, W. Wilkening, M. Baeumler, and F. Köhl, Phys. Rev. Lett. **59**, 240 (1987).
[9] I.T. Yoon, J.H. Leem, and T.W. Kang, J. Appl. Phys. **93**, 2544 (2003).
[10] S.B. Zhang, S.H. Wei, and A. Zunger, Phys. Rev. Lett. **78**, 4059 (1997); S.B. Zhang, S.H. Wei, A. Zunger, and H. Katayama-Yoshida, Phys. Rev. B **57**, 9642 (1998); Chris G. Van de Walle, Phys. Rev. Lett. **85**, 1012 (2000).
[11] G. Makov and M.C. Payne, Phys. Rev. B **51**, 4014 (1995).
[12] *Semiconductors Basic Data*, edited by O. Madelung (Springer-Verlag, Berlin, 1996).
[13] J. Ihm, A. Zunger, and M.L. Cohen, J. Phys. C **12**, 4409 (1979).
[14] D. Vanderbilt, Phys. Rev. B **41**, 7892 (1990).
[15] J.P. Perdew and Y. Wang, Phys. Rev. B **45**, 13244 (1992).
[16] Our results for the 64-atom cell compare reasonably well with earlier work of Erwin and Petukhov (Ref. 6) for substitutional and interstitial Mn in GaAs using a 54-atom cell. For example, the difference between the formation energies of Mn_i^{2+} and Mn_{Ga}^0 with $\epsilon_F=0$ that we find is 0.38 under As-rich conditions, while they obtain 0.44 for their 54-atom cell. Further they find Mn_i related $(+/2+)$ and $(0/+)$ transitions at ϵ_F of 0.66 and 0.98 eV, while we get 0.72 and 1.23 eV, respectively.
[17] G. Kresse and J. Furthmüller, Phys. Rev. B **54**, 11169 (1996); G. Kresse and J. Furthmüller, Comput. Mater. Sci. **6**, 15 (1996).
[18] The GGA optimized lattice constant for GaAs at the plane-wave basis cutoff of 13.3 Ry was 5.728 Å, to be compared with the experimental value of 5.65 Å, while the value using the LDA (Ref. 19) exchange functional is 5.601 Å.
[19] J.P. Perdew and A. Zunger, Phys. Rev. B **23**, 5048 (1981).
[20] Mn has a complex antiferromagnetic ground state which we have not considered in this work. Considering the antiferromagnetic fcc structure for Mn will decrease the formation energy of MnAs by 0.14 eV.
[21] P. Mahadevan and A. Zunger (unpublished).
[22] B. Clerjaud, J. Phys. C **18**, 3615 (1985).
[23] S.J.C.H.M. van Gisbergen, M. Godlewski, T. Gregorkiewicz, and C.A.J. Ammerlaan, Phys. Rev. B **44**, 3012 (1991).
[24] S.R. Shinde, S.B. Ogale, S. Das Sarma, J.R. Simpson, H.D. Drew, S.E. Lofland, C. Lanci, J.P. Buban, N.D. Browning, V.N. Kulkarni, J. Higgins, R.P. Sharma, R.L. Greene, and T. Venkatesan, cond-mat/0203576 (unpublished).
[25] V. Ossiniy, A. Jedrzejczak, M. Arciszewska, W. Dobrowolski, T. Story, and J. Sadowski, Acta Phys. Pol. A **100**, 327 (2001).
[26] R. Shioda, K. Ando, T. Hayashi, and M. Tanaka, Phys. Rev. B **58**, 1100 (1998).
[27] S.J. Potashnik, K.C. Ku, S.H. Chun, R.F. Wang, M.B. Stone, N. Samarth, and P. Schiffer, cond-mat/0212260 (unpublished).
[28] F. Matsukara, H. Ohno, A. Shen, and Y, Sugawara, Phys. Rev. B **57**, R2037 (1998).
[29] I. Kuryliszyn, T. Wojtowicz, X. Liu, J.K. Furdyna, and W. Dobrowolski, cond-mat/0207354 (unpublished).